Weierstraß–Institut
für Angewandte Analysis und Stochastik

im Forschungsverbund Berlin e.V.

Preprint ISSN 0946 – 8633

Flow instabilities in granular media due to porosity inhomogeneities

Theo Wilhelm[1], Krzysztof Wilmański[2]

submitted: 19th January 2001

[1] Institute for Geotechnics
and Tunnelling
University of Innsbruck
Technikerstrasse 13
A–6020 Innsbruck
Austria
E-Mail: theo.wilhelm@uibk.ac.at

[2] Weierstrass Institute
for Applied Analysis
and Stochastics
Mohrenstrasse 39
D–10117 Berlin
Germany
E-Mail: wilmansk@wias-berlin.de

Preprint No. 633
Berlin 2001

1991 *Mathematics Subject Classification.* 86-99, 76E20, 73Q05, 76S05, 76T05.

Key words and phrases. Piping, channeling, flow instability in granular materials (fluidization), multicomponent model of saturated soils.

Edited by
Weierstraß–Institut für Angewandte Analysis und Stochastik (WIAS)
Mohrenstraße 39
D — 10117 Berlin
Germany

Fax: + 49 30 2044975
E-Mail (X.400): c=de;a=d400-gw;p=WIAS-BERLIN;s=preprint
E-Mail (Internet): preprint@wias-berlin.de
World Wide Web: http://www.wias-berlin.de/

Abstract

The paper concerns a theoretical description of the piping phenomenon appearing in saturated sands at high filtration velocities. Motivated by own experiments we propose a thermodynamical two component model which accounts for a threshold effect at a critical value of the relative velocity of components. This property is incorporated in the source term of momentum balance equations by means of a nonlinear contribution accounting for spatial variations of the porosity. We prove the thermodynamical admissibility of such a model. By means of a linear stability analysis we show the existence of the onset of instability for realistic values of material parameters gained from experiments.

1 Introduction

We aim to construct a macroscopic model of water flows through sandy soils describing the loss of stability related to rapid changes of permeability. These changes are due to inhomogeneities of porosity which influence momentum exchange between components. In experiments one observes these phenomena in form of channels appearing in an initially homogeneous material. This leads, in turn, to local increments of flow velocities, fluidization and erosion take place destroying locally parts of the soil skeleton. Details concerning the physical motivation, experimental evidence, and geophysical relevance can be found in the Ph.D.-Thesis of Theo Wilhelm [T.W.].

Such channeling processes in saturated granular media are of interest in various fields of application. Their consequences in geotechnical engineering are frequently disastrous. As an illustrative example the effect of piping on the "Baldwin Hills" reservoir is shown in figure 1.

Inspection of seepage experiments[1] (see: figure 2) in which water flows through a macroscopically homogeneous[2] grain skeleton of sand, reveals the following characteristic phenomena:

i) At fluid velocities small compared to the minimum fluidizing velocity[3] the macroscopic homogeneity is preserved. Porosity, permeability, and thus fluid flow rates remain constant throughout the system.

[1] In these experiments the pore water pressure at the bottom of a water saturated specimen is increased. The resulting fluid flow rate is measured.

[2] The terms *microscopic* and *macroscopic* are used in a continuum mechanical sense (e.g. [J.B.]).

[3] The minimum fluidizing velocity is the velocity at which the Terzaghi effective stress theoretically vanishes and the grain skeleton (theoretically) looses its strength. The hydraulic gradient is equal to the critical hydraulic gradient (see: [T.W.] for further details and references).

Figure 1: Piping failure at Baldwin Hills Reservoir, California 1963 (Cedergren, 1967)

ii) When the fluid velocity further increases macroscopic inhomogeneities in form of channels directed towards the flow direction begin to form. Flows in smaller channels are attracted by bigger ones (see: figure 3).

iii) When a big channel reaches the surface of the sample the flow behavior changes significantly. The flow rate increases rapidly and it is concentrated mainly within the big channel. Smaller channels form back or change their directions towards the main channel.

These observations suggest that the fluid/grain skeleton interactions are sensitive to spatial variations of the porosity. It is demonstrated in figure 4: The flow resistance in a conically formed pipe or pore channel is smaller towards the direction of the widening of the channel.

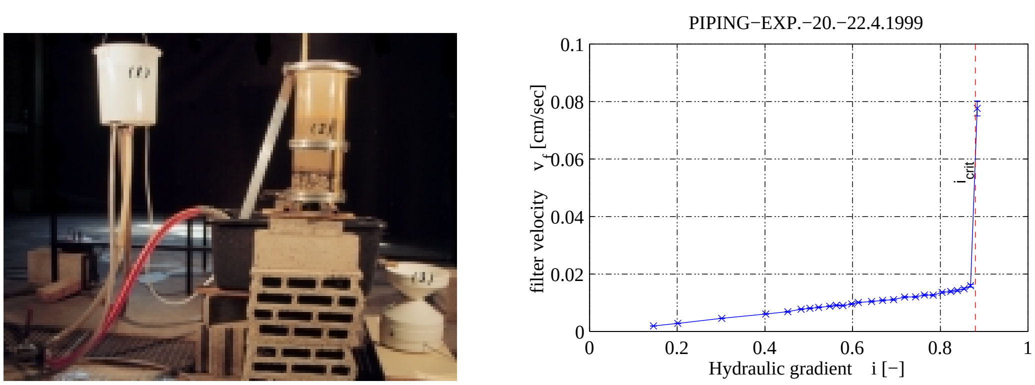

Figure 2: (a) Setup of seepage experiments (left) and (b) result of a seepage experiment with a quartz sand-water mixture (right). The course of the filter velocity nv^F against the applied pore water pressure gradient in terms of the hydraulic gradient $i := \partial_z p^F/(\rho^F g) - 1$ is shown.

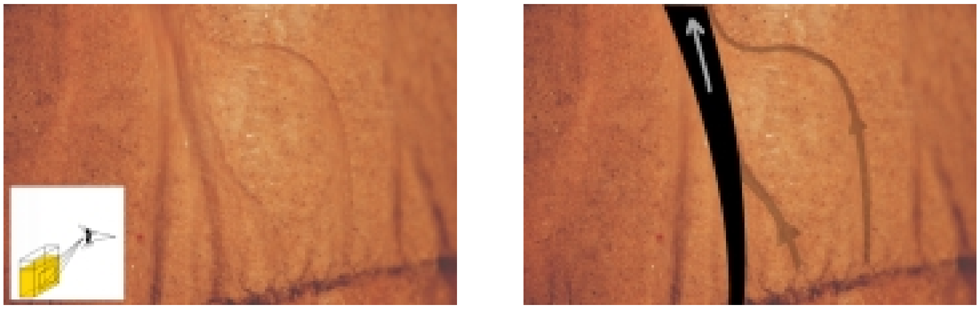

Figure 3: Pipe formation in seepage experiment. Picture from a seepage experiment: At high fluid velocities channels start to select a big channel (marked as a dark shadow on the right) for the flow in the direction to the top, while small channels are reoriented in direction of the big channel (light shadows on the right). The small picture in the box indicates the position of the camera, and the area of the experimental glass container reproduced in pictures.

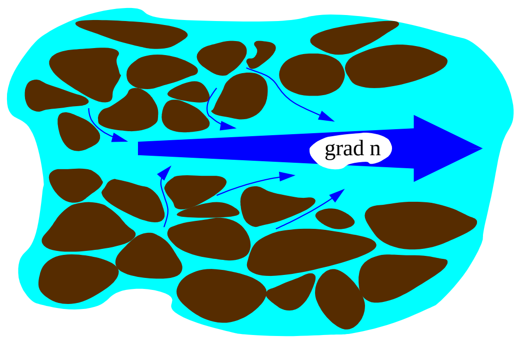

Figure 4: Flow in a conically shaped pore channel (schematic).

According to the above described observation we have to construct a model which yields an instability of flows appearing for sufficiently high porosity gradients, and sufficiently high relative velocities. We construct such a model by a modification of the momentum source appearing in two component models of saturated granular materials. In terms of models based on a Darcy law it means that we are modifying the Darcy law by making it dependent on the porosity gradient with a threshold behavior with respect to the relative velocity. Such a model must be necessarily nonlinear in its dependence on the relative velocity but not on the porosity gradient. We incorporate these requirements through a modification of the momentum source in the two component model. This requires a verification of thermodynamical conditions imposed on the model by the second law of thermodynamics. For this reason we devote a rather extensive second section of this paper to the evaluation of thermodynamical admissibility conditions.

We limit the attention to small elastic deformations of the skeleton. This limitation is not very crucial for the stability analysis shown in the third section, as it is performed by means of a linear perturbation method which is not influenced by mechanical nonlinearities within the stress tensor of the skeleton. We also assume the isotropy of the system, and neglect viscous effects in the partial stresses of the fluid component. All these assumptions are made in order to expose better the main property of the model yielding the instability of flows and piping effects.

In the third section we present the main results of the work. We investigate the stability of homogeneous seepage processes by superposing a small dynamical perturbation. We show that the dispersion relation may indeed contain solutions leading to the instability provided a material coefficient Γ which describes an influence of the porosity gradient on the exchange of momentum between components is sufficiently large. This result is illustrated by an example in the last section of the paper.

2 Construction of a macroscopical model

2.1 Fields and basic assumptions

We rely on a macroscopic two component description of saturated granular materials. Then in a continuum mechanical model processes are described by the following fields

$$(\mathbf{x},t) \mapsto \left\{\rho^S, \rho^F, n, u_k^S, v_k^F\right\}, \quad k=1,2,3, \tag{1}$$

where $\mathbf{x}$ denotes a current position of a particle of a solid component simultaneously occupied by a particle of the fluid component (continuous mixture), t is an instant of time and the fields are denoted as follows. ρ^S, ρ^F are the current mass densities of the solid and fluid component, respectively, $n \in [0,1]$ is the porosity (the volume fraction of the fluid component related to the total representative volume element, REV), u_k^S - the displacement of the solid, v_k^F - the velocity of the fluid. We use Cartesian coordinates $\left\{x^k\right\}_{k=1,2,3}$.

As we aim to describe solely certain stability properties of flows in such materials we neglect the compressibility of real materials. This yields some thermodynamical limitations as well as limitations of modes of propagation of waves. The former will be investigated in the sequel, the latter are immaterial for our present purposes. Consequently we make the following assumption

$$\rho^S = (1-n)\,\rho^{SR}, \quad \rho^{SR} = const., \qquad \rho^F = n\rho^{FR}, \quad \rho^{FR} = const., \tag{2}$$

where ρ^{FR}, ρ^{SR} are the so called "real" mass densities of components.

This assumption reduces the set of fields (1) to the fields of porosity n, displacement u_k^S, and velocity v_k^F.

We require that field equations should follow from balance laws of mass and momentum for both components supplemented with appropriate constitutive relations.

We limit attention to isotropic poroelastic materials and ideal fluids. We explain the physical contents of these assumptions in the next section.

It is obvious from the choice of fields that we consider solely isothermal processes, i.e. temperature will not appear anywhere in this model in the explicit form.

2.2 Field equations

As mentioned above we rely on partial balance equations for the two component system. Under the incompressibility assumption described in the previous section the mass balance equations reduce to the following form (e.g. [K.W.1])

$$\begin{aligned} \frac{\partial n}{\partial t} + \frac{\partial}{\partial x^k}\left(n v_k^F\right) &= 0, \quad \frac{\partial}{\partial x^k}\left[(1-n)\, v_k^S + n v_k^F\right] = 0, \\ v_k^S &:= \frac{\partial u_k^S}{\partial t}. \end{aligned} \tag{3}$$

On the other hand the partial momentum equations are as follows

$$\begin{aligned} \rho^S\left(\frac{\partial v_k^S}{\partial t} + v_l^S \frac{\partial v_k^S}{\partial x^l}\right) &= \frac{\partial T_{kl}^S}{\partial x^l} + p_k^*, \\ \rho^F\left(\frac{\partial v_k^F}{\partial t} + v_l^F \frac{\partial v_k^F}{\partial x^l}\right) &= \frac{\partial T_{kl}^F}{\partial x^l} - p_k^*, \end{aligned} \tag{4}$$

where we use the following notation: T_{kl}^F, T_{kl}^S - the partial Cauchy stress tensors, p_k^* - the momentum production (diffusion force, internal friction, etc.), v_k^F, v_k^S - the partial velocities. We have neglected body forces for simplicity. They do not influence thermodynamical considerations which we present in the next section, and they can be easily supplemented when needed in applications.

These equations become field equations if we specify constitutive relations. For the purpose of this work we choose the following set of constitutive variables

$$\mathfrak{V} := \left\{ n, \frac{\partial n}{\partial x^k}, e_{kl}, w_k \right\}, \tag{5}$$

where

$$\begin{aligned} e_{kl} &:= \frac{1}{2}\left(\frac{\partial u_k^S}{\partial x^l} + \frac{\partial u_l^S}{\partial x^k}\right) \equiv \frac{\partial u_{(k}^S}{\partial x^{l)}}, \quad w_k := v_k^F - v_k^S, \\ \|e_{kl}\| &\equiv \max\left(\left|\lambda_e^1\right|, \left|\lambda_e^2\right|, \left|\lambda_e^3\right|\right) \ll 1, \end{aligned} \tag{6}$$

denote the deformation tensor of the solid component (skeleton), and the relative velocity, respectively. The deformation of the skeleton is assumed to be small, i.e. the biggest absolute value of the eigenvalues λ_e of e_{kl} is much smaller than unity.

The above choice of constitutive variables justifies the names of components mentioned in section 2.1. In the limit case $n = 0$ we deal with a linear elastic material, and in the limit case $n = 1$ we deal with an ideal (incompressible) fluid.

The following constitutive quantities must be specified

$$\mathfrak{C} := \left\{ T^F_{kl}, T^S_{kl}, p^*_k, \psi^F, \psi^S \right\}, \tag{7}$$

where ψ^F, ψ^S are the partial Helmholtz free energies. They are introduced below for thermodynamical reasons.

For these quantities we assume that the following constitutive relation holds

$$\mathfrak{C} = \mathfrak{C}\left(\mathfrak{V}\right). \tag{8}$$

It is assumed to be sufficiently smooth.

Substitution of constitutive relations in the balance equations yields field equations of the model.

2.3 Thermodynamical admissibility of constitutive relations

It is customary to require in continuous models that a second law of thermodynamics is satisfied by all solutions of field equations. For the class of isothermal processes considered in this work we assume this law to have the following form (e.g. [K.W.1])

$$\rho^S \left(\frac{\partial \psi^S}{\partial t} + v^S_k \frac{\partial \psi^S}{\partial x^k} \right) + \rho^F \left(\frac{\partial \psi^F}{\partial t} + v^F_k \frac{\partial \psi^F}{\partial x^k} \right) + \\ -T^S_{kl} \frac{\partial v^S_k}{\partial x^l} - T^F_{kl} \frac{\partial v^F_k}{\partial x^l} - p^*_k w_k \leq 0. \tag{9}$$

The second law is usually formulated as an entropy inequality. It reduces to the above form under the assumption of constant temperature. The Helmholtz free energies are introduced for convenience. If $\varepsilon^S, \varepsilon^F$ denote the densities of partial internal energies and η^S, η^F - the densities of partial entropies then

$$\psi^S := \varepsilon^S - T\eta^S, \quad \psi^F := \varepsilon^F - T\eta^F. \tag{10}$$

It is customary to eliminate the restriction of the inequality (9) to solutions of field equations by means of Lagrange multipliers (e.g. [I.M., K.W.2]). By doing so we obtain the following inequality which should hold for all fields

$$\rho^S \left(\frac{\partial \psi^S}{\partial t} + v^S_k \frac{\partial \psi^S}{\partial x^k} \right) + \rho^F \left(\frac{\partial \psi^F}{\partial t} + v^F_k \frac{\partial \psi^F}{\partial x^k} \right) + \\ -T^S_{kl} \frac{\partial v^S_k}{\partial x^l} - T^F_{kl} \frac{\partial v^F_k}{\partial x^l} - p^*_k w_k +$$

$$-\Lambda\left(\frac{\partial n}{\partial t}+\frac{\partial}{\partial x^k}\left(nv_k^F\right)\right)-\lambda\left(\frac{\partial}{\partial x^k}\left[\left(1-n\right)v_k^S+nv_k^F\right]\right)+$$

$$-\Lambda_k^F\left\{\rho^F\left(\frac{\partial v_k^F}{\partial t}+v_l^F\frac{\partial v_k^F}{\partial x^l}\right)-\frac{\partial T_{kl}^F}{\partial x^l}+p_k^*\right\}+$$

$$-\Lambda_k^S\left\{\rho^S\left(\frac{\partial v_k^S}{\partial t}+v_l^S\frac{\partial v_k^S}{\partial x^l}\right)-\frac{\partial T_{kl}^S}{\partial x^l}-p_k^*\right\}\leq 0. \tag{11}$$

Lagrange multipliers $\Lambda, \lambda, \Lambda_k^F, \Lambda_k^S$ are functions of constitutive variables $\mathfrak{V}$.

After application of the chain rule of differentiation in the inequality (11) the linearity with respect to some derivatives can be seen. This yields the condition that coefficients of these derivatives must vanish identically. We obtain for the coefficients of time derivatives:

$$\frac{\partial n}{\partial t}: \qquad \Lambda=\rho^S\frac{\partial\psi^S}{\partial n}+\rho^F\frac{\partial\psi^F}{\partial n}, \tag{12}$$

$$\frac{\partial}{\partial t}\frac{\partial n}{\partial x^k}: \qquad \frac{\partial}{\partial\frac{\partial n}{\partial x^k}}\left(\rho^S\psi^S+\rho^F\psi^F\right)=0, \tag{13}$$

$$\frac{\partial v^F}{\partial t}: \qquad \rho^F\Lambda_k^F=\frac{\partial}{\partial w_k}\left(\rho^S\psi^S+\rho^F\psi^F\right), \tag{14}$$

$$\frac{\partial v^S}{\partial t}: \qquad \rho^S\Lambda_k^S=-\frac{\partial}{\partial w_k}\left(\rho^S\psi^S+\rho^F\psi^F\right). \tag{15}$$

Consequently

$$\rho^F\Lambda_k^F=-\rho^S\Lambda_k^S. \tag{16}$$

and, according to relation (13), multipliers Λ_k^F, Λ_k^S are independent of the gradient $\frac{\partial n}{\partial x_k}$.

On the other hand the coefficients of spatial derivatives lead to identities[4]**:**

$$\frac{\partial v_k^S}{\partial x^l}: \qquad T_{kl}^S=-\left(1-n\right)\lambda\delta_{kl}+\frac{\partial}{\partial e_{kl}}\left(\rho^S\psi^S+\rho^F\psi^F\right)+$$

$$-\rho^F\frac{\partial\psi^F}{\partial w_k}w_l-\frac{\partial T_{ml}^S}{\partial w_k}\Lambda_m^S-\frac{\partial T_{ml}^F}{\partial w_k}\Lambda_m^F, \tag{17}$$

$$\frac{\partial v_k^F}{\partial x^l}: \qquad T_{kl}^F=-n\lambda\delta_{kl}-n\left(\rho^S\frac{\partial\psi^S}{\partial n}+\rho^F\frac{\partial\psi^F}{\partial n}\right)\delta_{kl}+$$

[4] the time derivative $\frac{\partial e_{kl}}{\partial t}$ gives only a subclass of the conditions quoted below due to the relation $\frac{\partial e_{kl}}{\partial t}=\frac{1}{2}\left(\frac{\partial v_k^S}{\partial x^l}+\frac{\partial v_l^S}{\partial x^k}\right)$.

$$-\rho^S \frac{\partial \psi^S}{\partial w_k} w_l + \frac{\partial T^S_{ml}}{\partial w_k} \Lambda^S_m + \frac{\partial T^F_{ml}}{\partial w_k} \Lambda^F_m, \tag{18}$$

$$\frac{\partial^2 n}{\partial x^k \partial x^l} : \qquad \frac{\partial}{\partial \frac{\partial n}{\partial x^{(k}}} \left(\rho^S \psi^S w_{l)} - \Lambda^S_m T^S_{l)m} - \Lambda^F_m T^F_{l)m} \right) = 0, \tag{19}$$

where the condition (13) was applied.

The condition following from the linearity with respect to the derivative $\frac{\partial e_{kl}}{\partial x^m}$ is immaterial for further considerations, and we shall not quote it here.

It remains the following nonlinear part of the inequality which is called the residual inequality:

$$\left(\rho^S \frac{\partial \psi^S}{\partial n} + \lambda \right) w_k \frac{\partial n}{\partial x^k} + \left(w_k + \Lambda^F_k - \Lambda^S_k \right) p^*_k \geq 0. \tag{20}$$

It defines the dissipation in processes.

Let us notice that the dissipation contains an explicit dependence on the Lagrange multiplier λ. This multiplier plays the role of the reaction force on the constraint following from the assumption on incompressibility of real components (compare [K.W.1]). Consequently it should be determined by field equations rather than by a constitutive relation, and it should not appear in the dissipation inequality as the constraint $(3)_2$ is holonomous (i.e. nondissipative). Hence the inequality (20) cannot contain linear contributions of the porosity gradient, and this yields the necessity of dependence of the momentum source on this gradient.

We do not investigate the above results in their full generality, and proceed to simplifications yielding a model sufficient for our purposes.

We assume the system to be *isotropic, and linear with respect to a dependence on the porosity gradient* $\frac{\partial n}{\partial x^k}$. This means that neither free energies ψ^S, ψ^F, nor partial stress tensors T^S_{kl}, T^F_{kl}, may depend on the porosity gradient. Then the identities (13), and (19) are identically satisfied. Simultaneously we have the following representation for the momentum source (an isotropic vector function of two vectorial constitutive variables)

$$p^*_k = \Pi w_k + \nu \frac{\partial n}{\partial x^k} + \theta \varepsilon_{klm} w_l \frac{\partial n}{\partial x^m}, \tag{21}$$

where Π, ν, θ are scalar functions of invariants: $W := \frac{1}{2} w_k w_k$, and $w_k \frac{\partial n}{\partial x^k}$. ε_{klm} is the permutation symbol. Substitution in (20) yields

$$\left[\lambda + \nu + \rho^S \frac{\partial \psi^S}{\partial n} + \nu \left(\frac{1}{\rho^F} + \frac{1}{\rho^S} \right) \frac{\partial}{\partial W} \left(\rho^S \psi^S + \rho^F \psi^F \right) \right] w_k \frac{\partial n}{\partial x^k} +$$
$$+ \Pi \left[1 + \left(\frac{1}{\rho^F} + \frac{1}{\rho^S} \right) \frac{\partial}{\partial W} \left(\rho^S \psi^S + \rho^F \psi^F \right) \right] w_k w_k \geq 0. \tag{22}$$

We have used here the identity (13), and, in addition, we left out the dependence on nonlinear invariants containing contributions of e_{kl}. The latter simplification is due to the assumption (6).

Apparently the contribution with the coefficient θ does not appear in the dissipation inequality (22). It means its sign can be arbitrary as far as the thermodynamical admissibility is concerned. However this contribution to momentum balance equations seems to yield vibrations whose physical meaning is at least unclear. For this reason we assume in this work $\theta \equiv 0$.

According to the previous remarks we have to choose ν in such a way that the contribution of λ to (22) disappears. We proceed to investigate this problem.

The linearity with respect to the porosity gradient, and the assumption that λ is a field yield:

$$\lambda + \nu + \rho^S \frac{\partial \psi^S}{\partial n} = 0, \qquad \frac{\partial}{\partial W}\left(\rho^S \psi^S + \rho^F \psi^F\right) = 0. \tag{23}$$

On the other hand in static processes ($v_k^F = 0, v_k^S = 0$) the momentum balance of the fluid $(4)_2$, and relation (18) yield:

$$-\frac{\partial p^F}{\partial x^k} - \nu|_{w_k=0} \frac{\partial n}{\partial x^k} = 0, \quad p^F := n\left(\lambda + \left(\rho^S \frac{\partial \psi^S}{\partial n} + \rho^F \frac{\partial \psi^F}{\partial n}\right)\Bigg|_{w_k=0}\right). \tag{24}$$

Simultaneously we expect in this case that the pore water pressure p and the partial pressure in the fluid p^F are related to each other: $p^F = np$ [J.B.]. On the other hand the expression in parenthesis of $(24)_2$ cannot be constant in general as the free energies depend, for instance, on the deformation e_{kl}. Consequently, the above relation for the partial pressure, and the fact that the pore water pressure p is constant in such static experiments we must require:

$$p = -\left.\nu\right|_{w_k=0}, \quad \left(\rho^S \frac{\partial \psi^S}{\partial n} + \rho^F \frac{\partial \psi^F}{\partial n}\right)\Bigg|_{w_k=0} = 0, \quad \lambda = p. \tag{25}$$

It follows from $(23)_1$

$$\rho^S \frac{\partial \psi^S}{\partial n}\bigg|_{w_k=0} = 0. \tag{26}$$

We proceed to specify constitutive relations for partial stresses T_{kl}^F, T_{kl}^S, and the contribution $\nu \frac{\partial n}{\partial x_k}$ to the momentum source.

For the latter we make the following assumption motivated by the results for the dependence of free energies on the porosity in the static case $(25)_2$

$$\rho^S \frac{\partial \psi^S}{\partial n} = -\rho^F \frac{\partial \psi^F}{\partial n} = \frac{\Gamma}{\sqrt{2}}\left(1 + \frac{W - Y}{|W - Y|}\right)\sqrt{W}, \quad \Gamma, Y > 0, \tag{27}$$

where the material parameter Γ may be still dependent on the porosity n, deformation of the skeleton e_{kl}, and the invariant of the relative velocity W. The expression in parenthesis introduces the threshold behavior into the model. Its existence has been indicated in the introduction (see figure 2b). The constant $\sqrt{2Y}$ denotes the threshold. As we see further it yields flow instabilities for relative velocities whose magnitude exceeds the limit $\sqrt{2Y}$. It needs to be determined experimentally, however, in a first approximation it can be set equal to the minimum fluidizing velocity.

For the partial stress tensors T^S_{kl}, T^F_{kl} we assume in addition that they do not contain contributions of the relative velocity w_k. Otherwise we would have some sort of viscid reactions of the material which we excluded from the beginning of the construction of the model. Inspection of relations (17), (18) shows that such contributions would be of the order higher than one in w_k. Such an assumption together with (27) yields the following constitutive relations:

$$
\begin{aligned}
T^S_{kl} &= -(1-n)\,p\delta_{kl} + \frac{\partial}{\partial e_{kl}}\left(\rho^S\psi^S + \rho^F\psi^F\right), \qquad (28)\\
T^F_{kl} &= -np\delta_{kl}.
\end{aligned}
$$

In addition the assumption on small deformations of the isotropic skeleton yields Hooke´s relation in the partial stress T^S_{kl}

$$
\frac{\partial}{\partial e_{kl}}\left(\rho^S\psi^S + \rho^F\psi^F\right) = \lambda^S e_{mm}\delta_{kl} + 2\mu^S e_{kl}, \qquad (29)
$$

where λ^S, μ^S are Lamé parameters dependent solely on the porosity n.

The momentum balance equations (4) have then the following form

$$
\begin{aligned}
\rho^S\left(\frac{\partial v^S_k}{\partial t} + v^S_l\frac{\partial v^S_k}{\partial x^l}\right) &= -(1-n)\frac{\partial p}{\partial x^k} + \frac{\partial}{\partial x^l}\left(\lambda^S e_{mm}\delta_{kl} + 2\mu^S e_{kl}\right) + \\
&\quad + \Pi w_k - \frac{\Gamma}{\sqrt{2}}\left(1 + \frac{W-Y}{|W-Y|}\right)\sqrt{W}\frac{\partial n}{\partial x^k}, \qquad (30)
\end{aligned}
$$

$$
\rho^F\left(\frac{\partial v^F_k}{\partial t} + v^F_l\frac{\partial v^F_k}{\partial x^l}\right) = -n\frac{\partial p}{\partial x^k} - \Pi w_k + \frac{\Gamma}{\sqrt{2}}\left(1 + \frac{W-Y}{|W-Y|}\right)\sqrt{W}\frac{\partial n}{\partial x^k},
$$

$$
\lambda^S, \mu^S, \Pi, \Gamma, Y > 0.
$$

In the remaining part of this work we investigate linear stability properties of processes described by these equations.

Relations (27) and (29) yield integrability relations

$$
\frac{\partial}{\partial e_{kl}}\left(\frac{\rho^F\psi^F}{n} - \frac{\rho^S\psi^S}{1-n}\right) = \frac{\partial}{\partial n}\left(\lambda^S e_{mm}\delta_{kl} + 2\mu^S e_{kl}\right), \qquad (31)
$$

which impose limitations of the dependence of material parameters λ^S, μ^S on the porosity n. For instance, if we assume that ψ^F is independent of e_{kl} we obtain a linear dependence on the porosity. This is a relatively good approximation for porosities between approximately 0.1 to 0.4. Otherwise we have to construct a model without, for instance, the requirement (27). Simultaneously the definition of Γ which is a part of relation (27) has consequences on the behavior of material parameters λ^S, μ^S. The above integrability conditions indicate that these parameters may change in a discontinuous manner at $W = Y$, i.e. by flows locally yielding fluidization. This is in accord with the remarks which we made in the introduction. We shall account for this property in the next section assuming that the elastic parameters become much smaller after fluidization.

3 Stability analysis

In this section a perturbation analysis for a saturated elastic grain skeleton subject to an upward fluid flow is shown. The nonlinear interaction term introduced in the previous section is taken into account. It is shown that the analysis is therefore capable to model experimentally observed instabilities that classical models are not able to describe.

3.1 Experimental observation

The stability of a (quartz) sand-water mixture at a critical upward fluid flow was investigated experimentally. A 20 cm high column of fine quartz sand contained in a perspex cylinder was used as specimen (see figure 2a). The pore water pressure at the bottom of the column was controlled and the outflux at the top was measured. The permeability and the relative fluid velocity were calculated from the geometry of the specimen, the applied pressure gradient and the water outflux. Figure 2b shows the filter velocity, $v_f := nv^F$, as a function of the applied pressure gradient in terms of the hydraulic gradient, $i := \partial_z p/(\rho^F g) - 1$ (the signs are due to the conventions that p is positive for compression and gravitation g is pointing towards the positive z-direction). At the rapid fluid velocity increasement shown in the figure a channel has formed. The system has lost stability.

3.2 Model

The calculation is based on the balance equations (3) and (30). Modelled is the vertical flow of water through a grain skeleton in a wide tube. Due to the boundary conditions (horizontal displacements are zero) the problem reduces to one dimension. Gravitation is considered in the calculation by adding appropriate source terms to the momentum balance equations, $\rho^S g$ in $(30)_1$ and $\rho^F g$ in $(30)_2$. It is assumed that the relative velocity has exceeded the threshold, $W > Y$, such that the nonlinear interaction term becomes active. In the one dimensional case only the components

T^F_{33}, T^S_{33} and e_{33} appear in the calculation (not quoted here). Thus the indices will be skipped (e.g. $e := e_{33}$).

3.3 Field equations

Together with the compatibility condition relating the motion of the skeleton to the deformation:

$$\partial_t e = \partial_z v^S \tag{32}$$

the equations for the fields $\{n, p, v^F, v^S, e\}$ are:

$$\begin{aligned}
\partial_t n + \partial_z \left[n v^F \right] &= 0 \\
-\partial_t n + \partial_z \left[(1-n) v^S \right] &= 0 \\
n\rho^{FR} \left[\partial_t v^F + v^F \partial_z v^F \right] &= -n\, \partial_z p + n\rho^{FR} g – \Pi(v^F – v^S) + \Gamma \left| v^F – v^S \right| \partial_z n \\
(1-n)\rho^{SR} \left[\partial_t v^S + v^S \partial_z v^S \right] &= E\, \partial_z e - (1-n)\partial_z p + (1-n)\rho^{SR} g + \\
&\quad + \Pi(v^F - v^S) - \Gamma \left| v^F - v^S \right| \partial_z n \\
\partial_t e &= \partial_z v^S
\end{aligned} \tag{33}$$

The elasticity parameter E of the grain skeleton is related to the Lamê parameters of the formula (29) by the classical relation $E = \lambda^S + 2\mu^S$. It is assumed to be constant in this linear analysis.

3.4 Ground state – homogeneous seepage

The stability of the uniform state of a granulate subject to an upward fluid flow is investigated. This state of uniform flow, indicated by the subscript 0, is characterized by:

$$\begin{aligned}
n(z,t) &= n_0 = \text{const} \\
v^S(z,t) &= v^S_0 = 0 \\
v^F(z,t) &= v^F_0 = \text{const} \\
p(z,t) &= p_0(z) \\
e(z,t) &= e_0 = -\frac{c_1}{E}\, z
\end{aligned} \tag{34}$$

The stress distribution in the grain skeleton follows to be a linear function of depth. From this and the constitutive relation for the skeleton, the deformation field for the ground state $(34)_5$ follows. The constant c_1 is positive, as stresses in the skeleton are defined negative for compression.

Substituting $(34)_{1-5}$ into the field equations reduces them to the equations governing the equilibrium:

$$0 = 0$$

$$
\begin{aligned}
0 &= 0 \\
-\partial_z\, p_0 + \rho^{FR} g - \frac{\Pi}{n_0} v_0^F &= 0 \\
-\frac{c_1}{1-n_0} - \partial_z\, p_0 + \rho^{SR} g + \frac{\Pi}{1-n_0} v_0^F &= 0 \\
0 &= 0
\end{aligned}
\tag{35}
$$

These equations describe a steady ground state. In the case of a velocity controlled system[5] the pore water pressure $p_0(z)$ and the deformation $e_0(z)$ can be calculated from these equations for a given fluid velocity v_0^F. In the case of a pressure gradient controlled system[6] the fluid velocity v_0^F and the deformation $e_0(z)$ can be calculated for a given pressure gradient.
If c_1 is set equal to the submerged unit weight of the skeleton, $\gamma_0^{'} := (1-n_0)(\rho^{SR} - \rho^{FR})g$, equations $(35)_{3-4}$ imply that v_0^F must vanish, thus describing the so called "geostatic" stress state consistently:

$$
\begin{aligned}
E e_0 &= -\gamma_0^{'}\, z \\
p_0 &= \rho^{FR}\, g\, z
\end{aligned}
\tag{36}
$$

3.5 Linear equations governing small perturbations

To study the stability of the steady ground state the fields $(34)_{1-5}$ are augmented by small perturbations (indicated by subscripts 1):

$$
\begin{aligned}
n(z,t) &= n_0 + n_1(z,t) \\
v^S(z,t) &= v_1^S(z,t) \\
v^F(z,t) &= v_0^F + v_1^F(z,t) \\
p(z,t) &= p_0(z) + p_1(z,t) \\
e(z,t) &= e_0(z) + e_1(z,t)
\end{aligned}
\tag{37}
$$

Substituting $(37)_{1-5}$ into the field equations $(33)_{1-5}$, linearizing and considering the relations for the equilibrium solutions, $(35)_{3-4}$, the linearized equations governing the perturbations follow as:

$$
\begin{aligned}
\partial_t n_1 + n_0 \partial_z v_1^F + v_0^F \partial_z n_1 &= 0 \\
-\partial_t n_1 + (1-n_0)\partial_z v_1^S &= 0 \\
n_0 \rho^{FR} \partial_t v_1^F &= -n_1 \partial_z p_0 - n_0 \partial_z p_1 + n_1 \rho^{FR} g + \\
&\quad -\Pi(v_1^F - v_1^S) + \Gamma\,|v_0^F|\,\partial_z n_1 \\
(1-n_0)\rho^{SR}\partial_t v_1^S &= E\,\partial_z e_1 - (1-n_0)\partial_z p_1 + n_1 \partial_z p_0 - n_1 \rho^{SR} g + \\
&\quad +\Pi(v_1^F - v_1^S) - \Gamma\,|v_0^F|\,\partial_z n_1 \\
\partial_t e_1 &= \partial_z v_1^S
\end{aligned}
\tag{38}
$$

[5]The fluid flow v_0^F is controlled in the experiment. The known porosity depends on the material used and the way the experiment is prepared.

[6]The pore fluid pressure gradient $\partial_z p_0$ is controlled in the experiment.

3.6 Solutions in the form of plane waves

The perturbations are assumed to be in the form of plane waves:

$$\begin{aligned} n_1(z,t) &= N e^{(st+ikz)} \\ v_1^S(z,t) &= V^S e^{(st+ikz)} \\ v_1^F(z,t) &= V^F e^{(st+ikz)} \\ p_1(z,t) &= P e^{(st+ikz)} \\ e_1(z,t) &= B e^{(st+ikz)} \end{aligned} \tag{39}$$

Here the amplitudes N, V^S, V^F, P, B are constant and k is the wave vector. It corresponds to the wavelength by $2\pi/|k|$. The factor s is in general complex, $s = a - ib$. The propagation velocity of the wave is $b/|k|$. The real part a determines the stability of the system. If it is negative or zero disturbances decay exponentially or remain small. The system is stable. If it is positive small disturbances grow exponentially with time.
Substituting the plane wave solutions $(39)_{1-5}$ into the governing equations for the small perturbations, $(38)_{1-5}$, these degenerate into five linear equations for the five unknowns $x_k := (n_1, v_1^S, v_1^F, p_1, e_1)$:

$$A_{jk} x_k = 0 \tag{40}$$

with:

$$A_{jk} = \begin{pmatrix} s + v_0^F ik & 0 & n_0 ik & 0 & 0 \\ -s & (1-n_0)ik & 0 & 0 & 0 \\ \partial_z p_0 - \rho^{FR} g - \Gamma\,|v_0^F|\,ik & -\Pi & n_0 \rho^{FR} s + \Pi & n_0 ik & 0 \\ -\partial_z p_0 + \rho^{SR} g + \Gamma\,|v_0^F|\,ik & (1-n_0)\rho^{SR} s + \Pi & -\Pi & (1-n_0)ik & -Eik \\ 0 & -ik & 0 & 0 & s \end{pmatrix}$$

This system of linear equations has nontrivial solutions if and only if the determinant of its coefficient matrix A_{jk} vanishes. This condition leads to dispersion relation (third order polynomial) for s as a function of k. Its roots determine all possible plane wave modes for a given wave vector k. They were calculated using the algebra package MAPLE. As the expressions are rather lengthy they are not quoted here. Depending on the parameters gained from experiments the real part of s might be greater than zero for some wave vectors k. These modes lead to an exponential increase in the amplitude of the originally small perturbations and thus to an instable behavior.

As parameters for the calculation values from the experiment presented in figure 2b close to its critical state were used:

$$\begin{aligned} \rho^{SR} &= 2650 \quad \mathrm{kg/m^3} \\ \rho^{FR} &= 1000 \quad \mathrm{kg/m^3} \\ n_0 &= 0.47 \end{aligned}$$

$$
\begin{aligned}
\Pi &= n_0^2 \rho^{FR} g / \kappa = 1.2 \cdot 10^7 \quad \mathrm{kg/(m^3\ s)} \\
v_0^F &= -1.6 \cdot 10^{-4} \quad \mathrm{m/s} \\
\partial_z p_0 &= \rho^{FR} g - \frac{\Pi}{n_0} v_0^F = 14085 \quad \mathrm{Pa/m}
\end{aligned}
$$

Here κ is the (DARCY) permeability evaluated from the experiment. The bulk modulus was assumed to be very small $E = 1.0$ Pa. This assumption is motivated by a dependence of the stiffness of sand from the mean stress. In the range well bellow the threshold the skeleton behaves in a rather stiff manner with values of material parameters different from those in the vicinity of the point of fluidization. However the ground state belongs to this vicinity. There the sand looses its stiffness. This is the reason for the choice of the small value of E. Such a dependence was indicated at the end of section 2.3.

Out of three roots figure (5) shows the significant root responsible for the unstable behaviour:

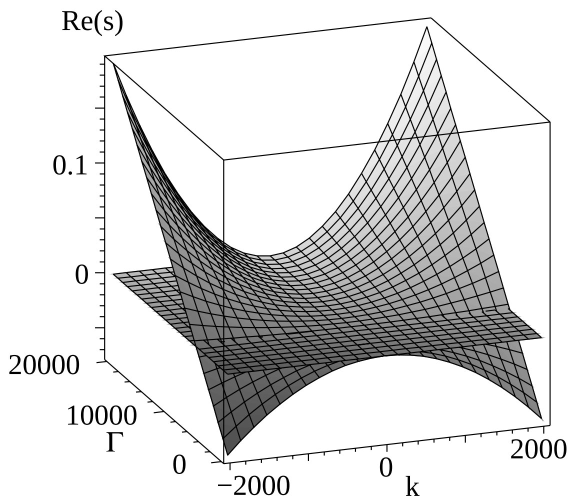

Figure 5: Real part of one of the three roots of the dispersion relation as a function of the wave number k, and the material parameter appearing in the nonlinear interaction Γ. Unstable modes can be seen ($Re(s) > 0$) can be seen for $\Gamma \gtrsim 6000$ kg/(m^2 s). The bulk modulus used in the calculation is $E = 1.0$ Pa.

The real part of s is plotted as a function of the wave number k and Γ, the parameter of the nonlinear interaction term. Regions where the real part of s is greater than zero represent unstable modes. It can be seen that there exist unstable modes for physically relevant parameters ($\Gamma > 0, E > 0$).

The instability of the system could be modelled using even the simplest form of the nonlinear interaction term. The same calculation omitting the nonlinear interaction (by setting $\Gamma = 0$) does not show unstable modes ($Re(s) > 0$) unless the bulk modulus E is set to unrealistic, negative values (not quoted here).

The above results show that the new model can be used for more realistic conditions of flows in soils in order to describe the fluidization phenomena and the accompanying creation of patterns.

4 Acknowledgements

This work was supported by the AUSTRIAN SCIENCE FUND (FWF) in the framework of the projects P10956-OETE and P12701-TEC.

5 References

[T.W.] THEO WILHELM; *Piping in Saturated Granular Media*, Ph.D.-Thesis, University of Innsbruck (2000),
ftp://ftp.uibk.ac.at/pub/uni-innsbruck/igt/publications/_wilhelm/phd_thesis_wilhelm.pdf.

[J.B.] JACOB BEAR; *Dynamics of Fluids in Porous Media*, Dover Publ., N.Y. (1972).

[I.M.] INGO MÜLLER; *Thermodynamics*, Pitman, N.Y. (1985).

[K.W.1] KRZYSZTOF WILMANSKI; Note on the Incompressibility in Theories of Porous and Granular Materials, ZAMM, **81**, (2001), 1, 37-42.

[K.W.2] KRZYSZTOF WILMANSKI; Thermomechanics of Continua, Springer, Berlin (1998).